Solution Conformations of a Peptide Containing the Cytoplasmic Domain Sequence of the β Amyloid Precursor Protein[†]

Christopher D. Kroenke,[‡] Dorota Ziemnicka-Kotula,[§] Jiliu Xu,[§] Leszek Kotula,*[,§] and Arthur G. Palmer, III*[,‡]

Department of Biochemistry and Molecular Biophysics, Columbia University, New York, New York 10032, and Laboratory of Molecular Neurobiology, New York State Institute for Basic Research in Developmental Disabilities, Staten Island, New York 10314

Received March 12, 1997; Revised Manuscript Received May 7, 1997[⊗]

ABSTRACT: The cytoplasmic domain of the β amyloid precursor protein (βAPP) may play a role in cellular events that lead to the secretion of the Aβ peptide, the major constituent of amyloid plaques found in the brains of individuals affected by Alzheimer's disease, by interacting with cellular factors involved in βAPP function or processing. In order to elucidate the structural basis of cytoplasmic domain activity, the conformations adopted in solution by a peptide containing the 47-residue C-terminal sequence of βAPP have been investigated by NMR and CD spectroscopy. The peptide does not have a stable tertiary structure, but local regions of the polypeptide chain populate defined conformations. In particular, the amino acid sequences TPEE and NPTY form type I reverse turns. These structured regions correspond to sequences within the cytoplasmic domain implicated in the biological activity of βAPP.

Cellular processing of the β amyloid precursor protein (βAPP)[1] generates the Aβ peptide, which is the major constituent of amyloid plaques found in the brains of individuals affected by Alzheimer's disease (Selkoe, 1996). As shown in Figure 1, βAPP resembles a cell surface receptor in its overall organization with a large extracellular domain, a single putative transmembrane region, and a 47-residue cytoplasmic tail (Kang et al., 1987). Proteolytic cleavage at sites within the extracellular domain, approximately 28 residues from the extracellular membrane surface, and at sites within the membrane-spanning region, approximately 14 residues from the extracellular membrane surface, results in the release of the 39−43 residue Aβ peptide into the cerebrospinal fluid or blood stream. Although the biological function of βAPP and the purpose of its extensive post-translational processing remain obscure, delineation of the relationship between the function and processing of βAPP, Aβ secretion, and amyloid plaque formation is crucial for a molecular etiology of Alzheimer's disease. To date, structural studies of βAPP have focused on the region composing the Aβ peptide. Solution NMR studies indicate that the N-terminal two-thirds of Aβ folds into an α helical structure in aqueous solution (Talafous et al., 1994). Peptides that contain segments of the C-terminal one-third of Aβ have been shown to be helical in the presence of detergents

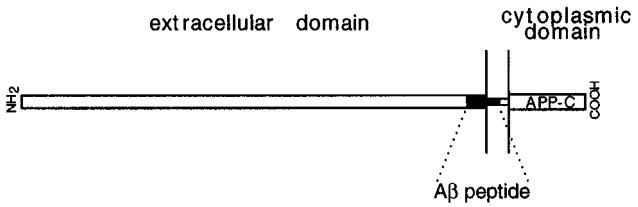

FIGURE 1: Organization of βAPP. The two vertical lines represent a phospholipid bilayer. The APP-C peptide contains the 47 carboxyl-terminal residues of βAPP and does not overlap with the Aβ peptide.

(Kohno et al., 1996). Solid state nuclear magnetic resonance (Lansbury et al., 1995), X-ray scattering (Kirschner et al., 1986), and Fourier transform infrared spectroscopy (Halverson et al., 1991) indicate that the C-terminal one-third of Aβ is extended in amyloid structures. Currently, intense efforts are devoted to uncovering the physical basis of conformational changes of Aβ (Lee et al., 1995) and relating the conformation adopted by this peptide *in vivo* to amyloid formation and the onset of Alzheimer's disease (Lansbury, 1996).

The cytoplasmic tail may play a role in βAPP function and pathology because specific sequences can serve as recognition sites for cytoplasmic factors or signals directing βAPP to subcellular compartments (Selkoe, 1994). Short amino acid sequences that adopt reverse turn conformations have been shown to act as determinants for internalization of cell surface receptors into endosomes [for a review, see Trowbridge et al. (1993)]. One class of these sequences are of the form NPXY, in which X designates any amino acid (Chen et al., 1990). Analysis of model peptides containing mutations in the NPVY sequence derived from the low-density lipoprotein (LDL) receptor internalization signal reveals that NPXY prefers to adopt a type I reverse turn conformation in solution (Bansal & Gierasch, 1991). The conformations of the sequence NPXY observed in proteins of known structure are biased in favor of solvent-exposed reverse turns (Collawn et al., 1990). In βAPP, the NPXY

[†] This work was supported by funds provided by the New York State Office of Mental Retardation (L.K.), National Institutes of Health Grants 2T32-GM08281 (C.D.K.), PO1-AG04220 awarded to Henry M. Wisniewski (D.Z.-K.), and R29-NS32874 (L.K.), an American Cancer Society Junior Faculty Research Award (A.G.P.), and an Irma T. Hirschl Career Scientist Award (A.G.P.).

* Authors to whom correspondence should be addressed.

[‡] Columbia University.

[§] New York State Institute for Basic Research in Developmental Disabilities.

[⊗] Abstract published in *Advance ACS Abstracts,* June 15, 1997.

[1] Abbreviations: βAPP, β amyloid precursor protein; Aβ, β amyloid peptide; NMR, nuclear magnetic resonance; CD, circular dichroism; TOCSY, total correlation spectroscopy; NOESY, nuclear Overhauser effect spectroscopy; HSQC, heteronuclear single-quantum coherence; TFE, trifluoroethanol; PTB domain, phosphotyrosine binding domain.

S0006-2960(97)00566-7 CCC: $14.00

motif is present in the functionally characterized internalization signal $_{681}$GYENPTY$_{687}$ [numbering refers to the sequence position in the βAPP$_{695}$ isoform (Kang et al., 1987)]. Deletion of $_{682}$YENPTY$_{687}$ abolishes internalization of βAPP from the plasma membrane in cell culture (Koo & Squazzo, 1994), while introduction of $_{681}$GYENPTY$_{687}$ into the cytoplasmic domain of an internalization-deficient mutant transferrin receptor restores internalization activity (Lai et al., 1995).

Normal βAPP functioning may require additional activities of the cytoplasmic domain. Several cytosolic factors that bind to the cytoplasmic domain of βAPP have been identified (Nishimoto et al., 1993; Fiore et al., 1995; Chow et al., 1996). In particular, the trimeric GTP-binding protein G_0 binds a peptide corresponding to 20 residues in the N-terminal half of the βAPP cytoplasmic domain (Nishimoto et al., 1993), and FE65 putatively recognizes the NPTY motif (Fiore et al., 1995; Guenette et al., 1996). Although potential physiological ligands for the extracellular domain of βAPP have not been reported, the similarity displayed with respect to other cell surface receptors raises the possibility that βAPP can transduce extracellular stimuli to the inside of a cell. In this scenario, interactions between the cytoplasmic domain and other signaling factors, such as G_0 and FE65, are an important part of normal βAPP function.

In order to gain further understanding of the structural basis for interactions between the βAPP cytoplasmic domain and other macromolecules, nuclear magnetic resonance (NMR) spectroscopy in aqueous solution and circular dichroism (CD) spectroscopy in mixed solvents have been used to investigate the conformations adopted by a 49-residue peptide, APP-C, that contains two N-terminal residues (Gly-Ser) fused to the 47-residue cytoplasmic domain sequence of βAPP. Although the peptide does not fold into a single stable structure, regions of the peptide preferentially adopt local conformations. These regions correspond to sequences within the cytoplasmic domain implicated in the above studies as internalization signals and determinants for binding of cytosolic factors.

MATERIALS AND METHODS

Expression and Purification of APP-C. The cytoplasmic domain of βAPP was expressed as a glutathione *S*-transferase (GST) fusion protein by subcloning DNA sequences encoding residues 649−695 of βAPP$_{695}$ (Robakis et al., 1987) into the pGEX expression vector (Pharmacia). The procedure for inserting the nucleotide sequence of βAPP into the expression vector involved the PCR amplification of the desired regions of the βAPP$_{695}$ cDNA using the specific 5′ and 3′ oligonucleotide primers, respectively: 5′ GTG GGA TCC AAG AAG AAA CAG TAC ACA TCC 3′ and 5′ CTG GAA TTC TAG ACT AGT TCT GCA TCT GCT C 3′. A *Bam*HI site was introduced into the 5′ primer, and an *Eco*RI site was introduced into the 3′ primer to facilitate unidirectional cloning into the pGEX-2T expression vector. A thrombin cleavage site was present between the βAPP and GST sequences. DH5α cells transformed with this plasmid were grown to log phase, and expression of the GST−APP-C fusion protein was induced with 0.1 mM IPTG. Three hours after induction, the bacteria were pelleted by centrifugation and lysed by sonication in 50 mM Tris buffer (pH 8.0) containing 1 mM EDTA, 1% Triton X-100, 1 mM PMSF, 2 μg/mL leupeptin, and 1 μg/mL pepstatin A. The water soluble fraction of the lysate was applied to a glutathione−Sepharose column equilibrated with phosphate-buffered saline (pH 7.3) (Sambrook et al., 1989) containing 1% Triton X-100, and the fusion protein was eluted with 5 or 20 mM glutathione. The purified fusion protein was cleaved with thrombin, and the peptide containing the cytoplasmic domain of βAPP (APP-C) was purified by gel filtration chromatography (Sephacryl S-100). The resulting 49-residue APP-C peptide contains two residues (Gly-Ser) from the thrombin cleavage site at the N terminus fused to the 47 C-terminal residues of βAPP. The peptide was exchanged into 20 mM sodium phosphate buffer (pH 6.3) and concentrated by ultrafiltration (Amicon) to final concentrations ranging from 1 to 4 mM. The sequence of APP-C was confirmed by N-terminal sequencing at the Institute for Basic Research in Developmental Diseases sequencing facility. ^{15}N-enriched APP-C was prepared by the procedure outlined above except that BL21 cells were grown on M9 minimal medium (Sambrook et al., 1989) containing $^{15}NH_4Cl$ as the sole nitrogen source.

NMR Spectroscopy. All NMR spectra were recorded on a Bruker AMX500 spectrometer using standard pulse sequences (Cavanagh et al., 1996) and the States−TPPI method of frequency discrimination (Marion et al., 1989b). APP-C samples for NMR spectroscopy were dissolved in 90% H_2O/10% D_2O buffer at pH 6.3 (20 mM sodium phosphate buffer and 0.05% sodium azide). Aside from spectra used to determine the temperature dependence of the H^N chemical shift, NMR spectra were recorded at 4 °C. Sample temperatures were calibrated with a 4% CH_3OH/96% CD_3OD sample and a calibration curve provided by Bruker Instruments. Two-dimensional homonuclear DQF-COSY (Rance et al., 1983), TOCSY (Bax & Davis, 1985), and NOESY (Bodenhausen et al., 1984) spectra were acquired with spectral widths of 5 kHz (9.8 Hz/point) in t_1 and 12.5 kHz (1.5 Hz/point) in t_2. TOCSY experiments utilized DIPSI-2 isotropic mixing (Shaka et al., 1988) with mixing times of 80 and 100 ms. The mixing time for the homonuclear NOESY experiment was 200 ms. Sensitivity-enhanced three-dimensional ^{15}N-edited TOCSY and ^{15}N-edited NOESY spectra (Palmer et al., 1992) were acquired with spectral widths of 7.14 kHz (27.9 Hz/point) in t_1, 1.05 kHz (8.2 Hz/point) in t_2, and 7.81 kHz (3.8 Hz/point) in t_3. Both of the pulse sequences used the PEP-Z modification (Akke et al., 1994) to eliminate relaxation differences between the two coherence transfer pathways. The ^{15}N-edited TOCSY experiment was recorded using the DIPSI-2 isotropic mixing sequence with a mixing time of 80 ms. The ^{15}N-edited NOESY experiment utilized a mixing time of 200 ms. HMQC−NOESY−HMQC spectra (Frenkiel et al., 1990; Ikura et al., 1990) were acquired with spectral widths of 1.05 kHz in t_1 and t_2 (4.1 and 8.2 Hz/point, respectively) and 7.81 kHz (3.8 Hz/point) in t_3. Mixing times were 100 and 200 ms. To measure the temperature dependence of the H^N chemical shift, 14 HSQC (Bodenhausen & Ruben, 1980) experiments were acquired at 4, 6, 8, 10, 12, 14, 16, 18, 20, 22, 24, 26, 28, and 30 °C with spectral widths of 1.05 kHz (8.2 Hz/point) in t_1 and 12.5 kHz (6.3 Hz/point) in t_2. Values for resolution in hertz per point are calculated for spectra following linear prediction, if used, and a single zero filling. Water suppression was obtained using presaturation for homonuclear experiments and high-power spin lock purge pulses (Messerle et al., 1989) for heteronuclear

experiments. Proton chemical shifts were referenced to dioxane (3.75 ppm), and nitrogen chemical shifts were referenced indirectly (Live et al., 1984; Bax & Subramanian, 1986).

Data sets were processed using Felix 2.30 (MSI) and in-house FORTRAN programs on a Silicon Graphics Indigo workstation. HSVD linear prediction (Barkhuijsen et al., 1987) was used to extend 2-fold the number of data points recorded in t_2 of the ^{15}N-edited TOCSY and NOESY spectra and in t_1 and t_2 of the HMQC−NOESY−HMQC spectra. Lorentzian-to-Gaussian window functions were applied in the acquisition dimension, and Kaiser window functions were applied in indirectly detected dimensions for all spectra except the DQF-COSY spectra. A 45°-shifted sine bell was applied in the acquisition dimension, and a 30°-shifted sine bell was applied in the indirect dimension of the DQF-COSY spectra. A digital low-pass filter was applied to all spectra to suppress the residual water signal (Marion et al., 1989a), and a fifth-order polynomial baseline correction was applied in the acquisition dimension of all spectra but the DQF-COSY spectra.

CD Spectroscopy. CD spectra were recorded at 4 °C on a JASCO J-600 spectropolarimeter using a 0.01 cm path length cuvette (Helma). Samples consisted of 71 μM APP-C with 0%, 9.7%, 19%, 29%, 48%, and 67% (v/v) trifluoroethanol (TFE), dissolved in 20 mM sodium phosphate buffer (pH 6.3) or 87% TFE (v/v) dissolved in 2 mM sodium phosphate buffer (pH 6.3). Each CD spectrum is an average of five scans with a 0.1 nm band width, a time constant of 1 s, and a step resolution of 0.1 nm. Concentrations of APP-C were determined by quantitative amino acid analysis (Columbia University Protein Chemistry Core Facility) and the percent α helicity was calculated as $[\theta]_{222}/[\theta]_{max} \times 100\%$, where $[\theta]_{max} = -39500(1 - 2.57/n)$ and n is the number of residues in the peptide (Chen et al., 1974).

RESULTS

Resonance Assignments. Resonance assignments for APP-C were obtained using the sequential assignment strategy (Wüthrich, 1986). Because severe overlap of H^N chemical shifts hindered resonance assignments using only two-dimensional homonuclear experiments, ^{15}N-edited NOESY and TOCSY experiments were used to assign most of the ^{15}N and ^{1}H nuclei in APP-C. HMQC−NOESY−HMQC experiments were used to resolve overlap between sequential H^N resonances. Figure 2 illustrates the increased dispersion of the ^{15}N chemical shifts compared with the limited dispersion of H^N chemical shifts. Chemical shifts are given in the Supporting Information. ^{15}N, H^N, H^α, H^β, and terminal methyl protons are essentially completely assigned from residues K_{651} to N_{695}. Overlap prevented the assignment of methylene protons beyond the H^β position for some of the long side chain amino acids. In addition, the four N-terminal residues could not be unambiguously assigned. H^β and H^γ resonances for P_{685} were assigned on the basis of the chemical shift patterns observed for prolines in a similar structural context (Dyson et al., 1988). The H^β and H^γ protons in P_{669} overlap with E_{670} side chain protons and therefore are unassigned.

Overall Structure. Short and medium range interresidue NOEs (Wüthrich, 1986) between H^N and H^α protons define the secondary structure adopted by APP-C in aqueous solution and are summarized in Figure 3. The observation of multiple sequential d_{NN} NOEs, as well as occasional $d_{NN}(i,i+2)$ and $d_{\alpha N}(i,i+2)$ NOEs and one $d_{\alpha N}(i,i+3)$ NOE between V_{663} and A_{666}, suggests that APP-C populates helical conformations. However, the absence of most medium range $d_{\alpha N}(i,i+3)$ and $d_{\alpha N}(i,i+4)$ NOEs indicates that stable α helices are not formed. In addition, all measured $^3J_{N\alpha}$ coupling constants between H^N and H^α protons (data not shown) lie in the range of 6.5−8 Hz, typical of conformationally averaged peptides; solvent exchange rates for all assigned backbone HN protons (data not shown) are within approximately 1 order of magnitude of the intrinsic rates in short random coil peptides (Bai et al., 1993), and a network of long range NOEs is not observed. These data further indicate that APP-C does not have a compact, stable, tertiary structure.

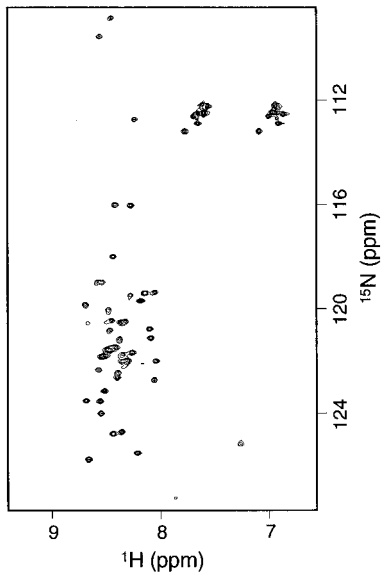

FIGURE 2: ^{1}H−^{15}N HSQC spectrum of APP-C at 4 °C and pH 6.3. All backbone H^N resonances are found within an approximately 1 ppm region, typical of disordered peptides.

Reverse Turns in APP-C. The most prominent structural features of APP-C are two type I reverse turns adopted by the sequences $_{668}$TPEE$_{671}$ and $_{684}$NPTY$_{687}$. The conformation of a type I reverse turn with a proline at position 2 is illustrated in Figure 4. NOEs important for identifying a type I reverse turn (Dyson et al., 1988) are expected for the H^N protons of positions 3 and 4 (2.3 Å), the position 3 H^N and the proline H^δ protons (1.9 and 3.5 Å), and position 4 H^N and proline H^δ protons (3.6 and 4.7 Å). The distances between the position 1 H^α and side chain protons of the position 3 and 4 H^N protons depend on the ψ and χ dihedral angles of position 1 but are generally within 5 Å, as determined by molecular modeling. Figure 5A shows experimental NOE data establishing that $_{668}$TPEE$_{671}$ forms a type I reverse turn: a strong NOE between E_{670} and E_{671} amide protons, a strong NOE between the E_{670} H^N and P_{669} H^δ protons, a weak NOE between the E_{671} H^N and the P_{669} H^δ protons, and NOEs between the T_{668} side chain H^γ protons and both the E_{670} and E_{671} amide protons. Expected cross-peaks to P_{669} H^β and H^γ resonances are not discernible due to spectral overlap. Additional NOEs are observed between the amide proton of T_{668} and the side chain H^β and H^γ protons of E_{671}. Finally, a long range NOE between the H^N proton of R_{672} and the methyl protons of V_{667} confirms that the

FIGURE 3: Summary of NMR results for APP-C. Sequential H^N-H^N and sequential $H^\alpha-H^N$ NOEs are designated by d_{NN} and $d_{\alpha N}$, respectively; H^N-H^N and $H^\alpha-H^N$ NOEs between residues i and $i+2$ are designated by $d_{NN}(i,i+2)$ and $d_{\alpha N}(i,i+2)$, respectively. The presence of an interresidue NOE cross-peak is indicated by a bar above the appropriate residues. The $I_{NN}/I_{\alpha N}$ ratios were determined from integrated d_{NN} and $d_{\alpha N}$ cross-peak volumes. Absolute amide proton temperature coefficients, $-\Delta\delta/\Delta T$, are given in units of parts per billion per kelvin.

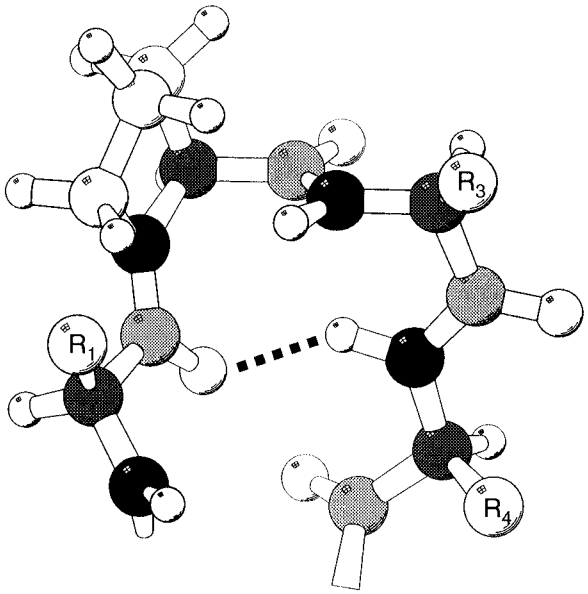

FIGURE 4: Conformation of a type I reverse turn with a proline at position 2. Backbone N^H, C^α, C', and O atoms are shown as large black, dark gray, light gray, and white spheres, respectively. Side chain carbon atoms are shown as large white spheres. Hydrogen atoms are shown as small white spheres. Residues are labeled R_1-R_4 on the C^β carbon (except for the proline). The dashed line represents a hydrogen bond between the H^N at position 4 and the carbonyl oxygen at position 1. The figure was drawn with Molscript (Kraulis, 1991).

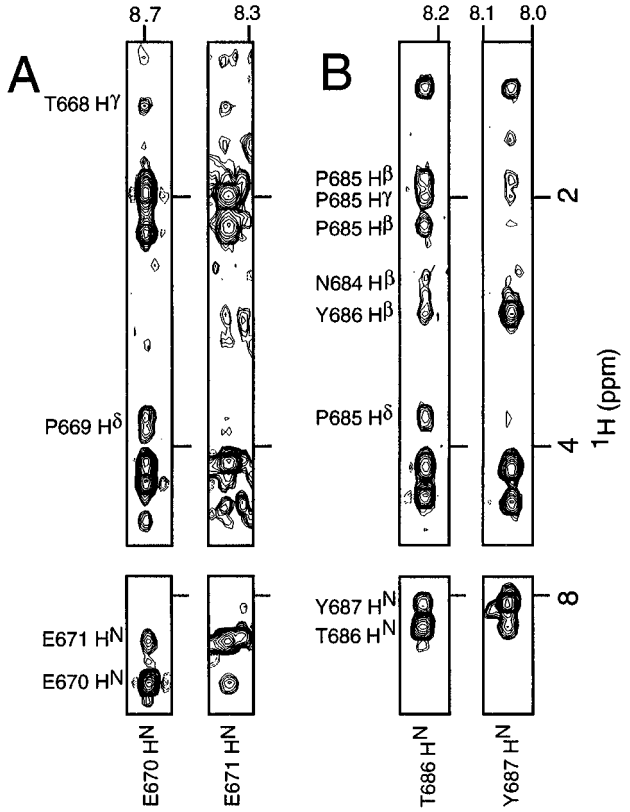

FIGURE 5: NOEs defining a type I reverse turn for (A) TPEE and (B) NPTY. Strips 0.1 ppm wide are taken from an ^{15}N-edited NOESY spectrum with a 200 ms mixing time. Strips containing cross-peaks to side chain and H^α protons are plotted at a lower contour level to show cross-peaks between proline H^δ and position 4 amide protons. Assignment of P_{685} H^β and H^γ resonances is based on the chemical shift patterns observed in Dyson et al. (1988).

peptide backbone reverses direction within the TPEE sequence.

As shown in Figure 5B, an analogous pattern of local NOEs is observed for the sequence $_{684}$NPTY$_{687}$: a strong NOE between the H^N protons of T_{686} and Y_{687}, strong NOEs between the T_{686} amide proton and P_{685} H^β, H^γ, and H^δ protons, weaker NOEs between Y_{687} H^N and the P_{685} side chain protons, NOEs between T_{686} H^N and N_{684} H^β protons, and weak NOEs (not readily apparent at the contour level plotted in Figure 5B) between Y_{687} H^N and N_{684} H^β protons. Again, medium range NOEs between the N_{684} H^N proton and Y_{687} H^α and H^β protons provide additional support for a reverse turn structure. In contrast to TPEE, long range NOEs between residues flanking the sequence NPTY are absent. However, NOEs are observed between the side chain amide protons of N_{684} and the backbone amide proton of Y_{687}. A cross-peak is also observed between the T_{686} H^N proton and one of the N_{684} side chain amide protons. These NOEs would not be expected if the conformation of NPTY was extended or random coil.

Amide−carbonyl hydrogen bond formation shields the amide proton from exchange with solvent molecules and reduces amide proton temperature coefficients, $-\Delta\delta/\Delta T$, for H^N protons participating in intramolecular hydrogen bonds compared to those for H^N protons hydrogen bonded to solvent. The random coil H^N temperature coefficients depend on the amino acid type but are generally larger than 6.5 ppb/K (Merutka et al., 1995). The absolute H^N temperature coefficients are shown in Figure 3 for APP-C residues where the chemical shift is linearly related to the temperature and the line width monotonically decreases as the temperature increases. The data are normalized to the temperature coefficients observed for random coil values and are plotted in Figure 6. As shown in Figure 4, the H^N proton of the fourth residue in a type I reverse turn forms a hydrogen bond

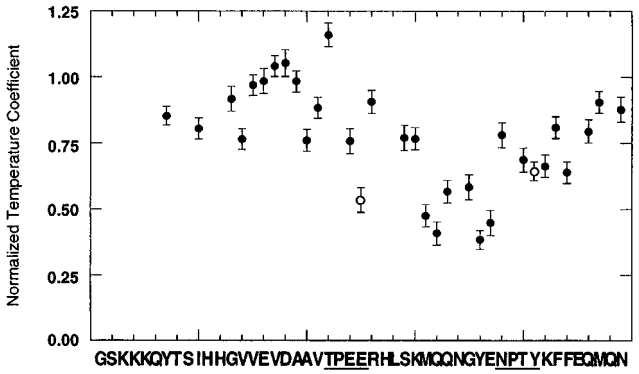

FIGURE 6: Normalized H^N temperature coefficients. The temperature coefficients (taken from Figure 3) are normalized to the intrinsic temperature dependence for each amino acid in a random coil conformation at pH 5 (Merutka et al., 1995) and graphed versus residue number. The two reverse turns are underlined in the peptide sequence, and the position 4 amide protons are plotted as open circles.

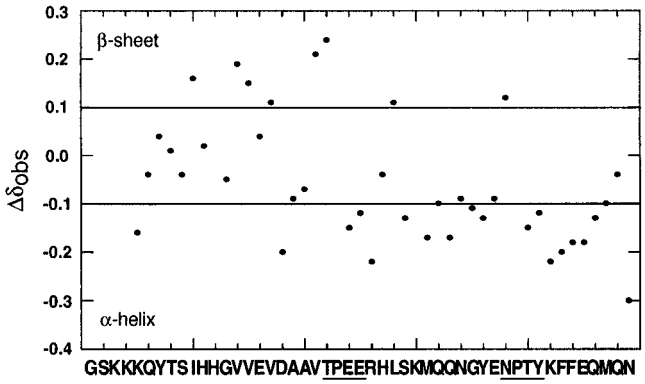

FIGURE 7: H^α secondary chemical shifts for APP-C. The differences, $\Delta\delta_{obs}$, between the observed chemical shifts, δ, and the random coil chemical shifts, δ_{rc}, are given as a function of sequence position. Consistent runs of sequential secondary shifts provide evidence for secondary structure (Wishart et al., 1992).

to the carbonyl oxygen of the first residue. Consequently, the H^N protons of E_{671} and Y_{687} are expected to form hydrogen bonds in the reverse turns. The normalized temperature coefficient for E_{671} is significantly reduced compared to those of neighboring residues. The Y_{687} amide proton temperature coefficient is smaller than those of most amide protons in APP-C, although the neighboring amide proton temperature coefficients are similarly reduced. Tyrosine has the largest value of $-\Delta\delta/\Delta T$ observed for amino acids in random coil peptides, and the aromatic side chains of Y_{682} and Y_{687} may perturb temperature coefficients for flanking residues (Merutka et al., 1995). The general tendency of reduced normalized temperature coefficients from residues M_{677} to F_{690} may reflect the presence of additional ordered structure and is discussed below.

The difference in the normalized temperature coefficients indicates that the hydrogen bond is stronger in the $_{668}$TPEE$_{671}$ reverse turn than in $_{684}$NPTY$_{687}$. The lack of long range NOEs between residues flanking $_{684}$NPTY$_{687}$, in combination with the decreased intensity of many of the medium range NOEs when compared to the analogous cross-peaks in the $_{668}$TPEE$_{671}$ turn, also suggest that the $_{668}$TPEE$_{671}$ reverse turn is more stable than that of $_{684}$NPTY$_{687}$.

Sequence Dependence of Helical Conformations. Short range NOEs typical of helical conformations are observed for backbone protons throughout the APP-C sequence. A large $I_{NN}/I_{\alpha N}$ cross-peak volume ratio indicates preferential population of helical conformations, although quantitative interpretation of the ratios is difficult in a highly dynamic peptide with potentially complex relaxation properties, such as APP-C. In particular, the average ^{15}N line width measured from a $^1H-^{15}N$ HSQC spectrum, which represents the mean of the relaxation rate constants for in-phase and anti-phase ^{15}N magnetization (Bax et al., 1990), is 4.6 Hz in the C-terminal half of APP-C (residues $E_{670}-N_{695}$), compared to 3.6 Hz for the N-terminal half (residues $K_{649}-E_{670}$). The average value of the $I_{NN}/I_{\alpha N}$ cross-peak volume ratio increases from 0.3 for residues $K_{649}-E_{670}$ to 0.5 for residues $E_{670}-N_{695}$. Although the value of this ratio is predicted to be larger than 0.5 in an ideal α helix, the relative increase of this ratio in the C-terminal half of APP-C indicates that helical conformations are more highly populated in this region of the peptide. If peptide backbone dihedral angles exchange only between ideal extended and ideal α helical conformations, and if the correlation times for cross relaxation are identical in helical and extended conformations, the fractional population of α helical conformations, f_α, is related to the ratio, $R = I_{NN}/I_{\alpha N}$, of the NOE intensities I_{NN} and $I_{\alpha N}$ by (Bradley et al., 1990)

$$f_\alpha = \frac{(1/r_{NN}^{\,6})_\beta - R(1/r_{\alpha N}^{\,6})_\beta}{R[(1/r_{\alpha N}^{\,6})_\alpha - (1/r_{\alpha N}^{\,6})_\beta] + (1/r_{NN}^{\,6})_\beta - (1/r_{NN}^{\,6})_\alpha} \quad (1)$$

where r_{ab} is the distance between protons a and b in an α helical or an extended (β) strand, as indexed outside of the parentheses. The sequential H^N-H^N and $H^\alpha-H^N$ distances are 2.8 and 3.5 Å for an ideal α helix, respectively, and 4.3 and 2.2 Å for an ideal β strand (Wüthrich, 1986). The average values obtained for f_α and f_β ($=1-f_\alpha$) are 0.57 and 0.43 for residues $K_{649}-E_{670}$ and 0.70 and 0.30 for residues $E_{670}-N_{695}$, respectively.

The average H^α secondary chemical shift, shown in Figure 7, provides a second sequence specific measurement of helical content. The average H^α secondary chemical shift, $\Delta\delta$, for amino acid residues in an α helix ($\Delta\delta_\alpha$) is -0.39 ppm, and that for a β strand ($\Delta\delta_\beta$) is 0.37 (Wishart et al., 1991). The average secondary shift for APP-C H^α protons from K_{649} to E_{670} ($\Delta\delta_{obs}$) is 0.03 ppm, whereas this value ($\Delta\delta_{obs}$) drops to -0.12 ppm for residues $E_{670}-N_{695}$. Assuming the backbone dihedral angles populate only ideal extended or α helical conformations, an estimation of f_α and f_β is provided by the relation

$$f_\alpha = \frac{\Delta\delta_{obs} - \Delta\delta_\beta}{\Delta\delta_\alpha - \Delta\delta_\beta} \quad (2)$$

which yields an f_α of 0.45 and an f_β of 0.55 for residues $K_{649}-E_{670}$, and an f_α of 0.64 and an f_β of 0.36 for residues $E_{670}-N_{695}$. Estimation of f_α using eq 2 does not require assumptions about local correlation times; however, the chemical shifts of protons are very sensitive to other effects, such as ring current shifts, that do not depend on backbone dihedral conformations.

A third experimental parameter sensitive to secondary structure formation is the H^N temperature coefficient (Figure 6). The average normalized values of $-\Delta\delta/\Delta T$ are 0.92 for the N-terminal half of APP-C and 0.69 for the C-terminal half of APP-C. The lowered temperature coefficients in the C-terminal half are consistent with transient intramolecular

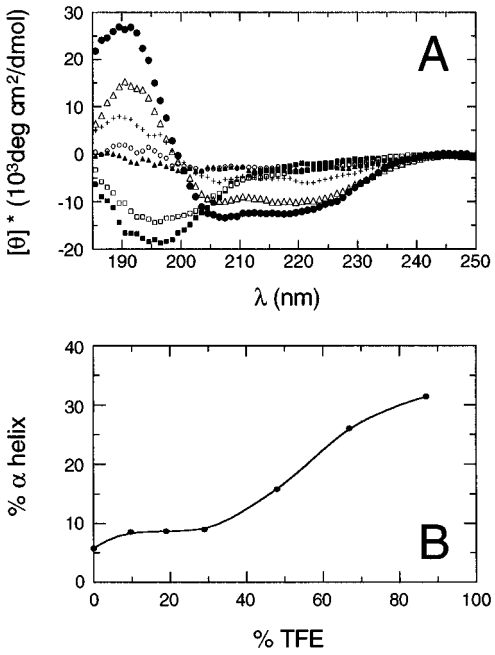

FIGURE 8: (A) CD spectra of APP-C. The TFE concentration is 0% (■), 9.7% (□), 19% (▲), 29% (○), 47% (+), 67% (△), and 87% (●). (B) Percent α helix calculated as described in Materials and Methods.

hydrogen bond formation that must accompany the preferential population of helical conformations; however, quantitative analysis of the temperature coefficients is not possible.

To further characterize helix formation in APP-C, CD spectra of the peptide were recorded at concentrations of aqueous TFE ranging from 0 to 87% (v/v). At 0% TFE, the spectrum is characteristic of a random coil, with a very low excess helical population of 6% (Figure 8A). As the TFE concentration increases, the decreasing molar ellipticity at 222 nm, $[\theta]_{222}$, is consistent with induction of increasing levels of helical structure in APP-C (Figure 8B). At 87% TFE, approximately 31% of APP-C is helical. The CD spectrum at 87% TFE exhibits features characteristic of α helices, including negative ellipticities at 206 and 222 nm and a band of positive ellipticity below 200 nm; however, qualitative differences also exist from the CD spectrum of an ideal α helix, such as the absence of a local maximum between 206 and 222 nm. Thus, TFE stabilizes α helix formation in the APP-C peptide, but other secondary structures may be stabilized as well. This result is consistent with the NMR results in that helix formation is favorable for only certain segments of the peptide. Indeed, stabilization of the $_{684}$NPTY$_{687}$ reverse turn may limit the extent of helix formation in TFE.

DISCUSSION

This report describes the conformations adopted by a peptide containing the βAPP cytoplasmic C-terminal sequence $K_{649}-N_{695}$. NMR and CD spectroscopy demonstrate that the peptide lacks stable tertiary structure in aqueous solution; however, networks of medium and long range NOEs are observed that constrain two sequences in the peptide, $_{668}$TPEE$_{671}$ and $_{684}$NPTY$_{687}$, to type I reverse turn conformations. Three NMR observables, the ratio of sequential backbone NOE intensities, the H^{α} chemical shift, and the H^{N} temperature coefficients, indicate that the populations of helical conformations are transient, but higher for the C-terminal half of the peptide, residues $E_{670}-N_{695}$, than for the N-terminal half, residues $K_{649}-E_{670}$.

Estimates of the population of helical conformations derived from NOE and chemical shift data are in agreement. The average results are $f_{\alpha} = 0.51$ in the N-terminal half of APP-C, consistent with random coil conformations, and $f_{\alpha} = 0.67$ in the C-terminal region, suggesting a population excess of helical conformations. Of course, the $_{684}$NPTY$_{687}$ sequence precludes formation of a contiguous α helix in the C-terminal half of APP-C, at least when the reverse turn conformation is populated. The low estimate of percent helix in aqueous solution obtained by CD spectroscopy agrees with the general absence of medium and long range NOEs characteristic of stable α helices. Thus, the populations of helical conformations detected by sequential backbone NOEs and H^{α} chemical shifts most likely reflects the random population of helical conformations by individual residues, rather than cooperative transitions to canonical α helical structures. CD spectroscopy suggests that these helical conformations are stabilized by TFE.

The sequence GYENPTY may play a direct role in βAPP metabolism by facilitating internalization of this protein from the cell surface (Koo & Squazzo, 1994; Lai et al., 1995). NMR spectroscopy demonstrates that the NPTY sequence within the APP-C peptide forms a significantly populated type I reverse turn in solution. The sequence NPXY frequently is present in the cytoplasmic domains of presumptive cell surface receptors with single transmembrane domains (Chen et al., 1990) and forms type I reverse turns in solution when incorporated into short peptides (Bansal & Gierasch, 1991; Backer et al., 1992). The sequence NPVY mediates internalization of the LDL receptor (Chen et al., 1990). Therefore, the present results suggest that the reverse turn formed by NPTY in APP-C is important for biological activities mediated by GYENPTY in βAPP.

A region of FE65 that is homologous to the phosphotyrosine binding (PTB) domain of Shc (Fiore et al., 1995; Guenette et al., 1996) has been suggested to recognize the $_{684}$NPTY$_{687}$ motif of βAPP. Binding assays (Zhou et al., 1996), screening of peptide libraries (Songyang et al., 1995), and yeast two-hybrid screens (He et al., 1995) have identified the sequence NPXpY (pY designates phosphotyrosine) and neighboring residues as being important for binding of various peptides to the PTB domains of Shc and IRS-1. Shc PTB domain binds with high affinity to phosphopeptides containing a hydrophobic residue five residues N-terminal to the phosphotyrosine (pY − 5), while the IRS-1 PTB domain binds preferentially to phosphopeptides with hydrophobic residues at positions at pY − 6 through pY − 8 (Wolf et al., 1995). In βAPP, the presence of the hydrophobic tyrosine residue at position 682, as well as the hydrophilic glutamine residue at position 679, is consistent with βAPP recognition by Shc-related PTB domains, such as FE65. However, evidence that Y_{687} is phosphorylated *in vivo* does not exist, and recent reports suggest phosphorylation of Y_{687} is not required for binding to FE65 (Zambrano et al., 1997). If the βAPP cytoplasmic tail is bound by a PTB domain in a manner similar to that of the reported high-resolution NMR structure of Shc complexed with a phosphopeptide derived from TrkA (Zhou et al., 1995), then the conformation adopted by the cytoplasmic tail would be different than the APP-C peptide free in solution. APP-C contains the requisite tight

turn at the sequence NPTY, even in the absence of phosphorylated tyrosine; however, the tendency of residues immediately N-terminal to NPTY to populate helical conformations in APP-C does not reflect the extended structure of the analogous residues in the peptide bound to Shc.

The sequence TPEE also adopts a reverse turn structure that may facilitate interactions between βAPP and cytosolic proteins. Specifically, Nishimoto et al. (1993) report that the trimeric GTP binding protein G_0 binds the βAPP cytoplasmic tail and that a 20-residue peptide including the TPEE sequence, but not GYENPTY, competes with full length βAPP for binding. This interaction has been implicated in a signal transduction cascade resulting in DNA fragmentation (Yamatsuji et al., 1996). Although the present results do not provide direct evidence for an interaction between TPEE and G_0, this turn constitutes the major region of nonrandom structure found in APP-C that overlaps with the 20-residue peptide defined by Nishimoto et al. (1993).

In native βAPP, the N terminus of the cytoplasmic tail is connected to the transmembrane domain (Figure 1). Whether the conformation of the cytoplasmic tail is stabilized or altered in proximity to the membrane surface is unknown. However, the presence of two reverse turn structures in regions of the cytoplasmic domain previously implicated in binding to other proteins suggests that the conformations observed in this study are similar to those adopted by at least the C-terminal half of the cytoplasmic domain of βAPP under physiological conditions. An α helix formed in the region spanning residues E_{670}−N_{695} would not have amphipathic character so stabilization of this structure by the membrane appears to be unlikely. If a stable helix were to be formed in the APP-C C terminus under physiological conditions, it should be noted that the N-terminal boundary of this helix would be the sequence $_{668}$TPEE$_{671}$. Although this sequence forms a type I reverse turn under the conditions used in this study, this amino acid sequence has a high propensity to form a "capping box" as described by Harper and Rose (1993). Because a type I reverse turn and an N-terminal helix cap are highly similar structures, possibly, a stable helix would be capped at its N terminus by the sequence $_{668}$TPEE$_{671}$. Random coil conformations are observed for the N-terminal 20 residues of APP-C in aqueous solution. Whether the N terminus provides a flexible spacer between the membrane and the reverse turns or whether this region adopts additional conformations that depend on the proximity to a membrane remains to be determined. The presence of short sequences with defined structures along a flexible chain in the cytoplasmic domain may contribute to βAPP trafficking and function by facilitating interactions with multiple cytosolic proteins.

ACKNOWLEDGMENT

We thank M. Akke (Columbia University), C. Bracken (Columbia University), and G. Merutka (Trimeris Inc.) for assistance with NMR and CD spectroscopy and for helpful discussions; W. A. Hendrickson (Columbia University) for use of the CD spectropolarimeter; and Henry M. Wisniewski, Marshall Elzinga, and David L. Miller (New York State Institute for Basic Research in Developmental Disabilities) for helpful discussions and suggestions regarding the manuscript. We thank Narayan Ramakrishna (IBR) for providing the plasmid containing the βAPP cDNA and Eirukur Benedikz (IBR) for technical assistance.

SUPPORTING INFORMATION AVAILABLE

One table containing chemical shift assignments (2 pages). Ordering information is given on any current masthead page.

REFERENCES

Akke, M., Carr, P. A., & Palmer, A. G. (1994) *J. Magn. Reson., Ser. B 104*, 298−302.
Backer, J. M., Shoelson, S. E., Weiss, M. A., Hua, Q. X., Cheatham, R. B., Haring, E., Cahill, D. C., & White, M. F. (1992) *J. Cell Biol. 118*, 831−839.
Bai, Y., Milne, J. S., Mayne, L., & Englander, S. W. (1993) *Proteins: Struct., Funct., Genet. 17*, 75−86.
Bansal, A., & Gierasch, L. M. (1991) *Cell 67*, 1195−1201.
Barkhuijsen, H., de Beer, R., & van Ormondt, D. (1987) *J. Magn. Reson. 73*, 553−557.
Bax, A., & Davis, D. G. (1985) *J. Magn. Reson. 65*, 355−360.
Bax, A., & Subramanian, S. (1986) *J. Magn. Reson. 67*, 565−569.
Bax, A., Ikura, M., Kay, L. E., Torchia, D. A., & Tschudin, R. (1990) *J. Magn. Reson. 86*, 304−318.
Bodenhausen, G., & Ruben, D. J. (1980) *Chem. Phys. Lett. 69*, 185−189.
Bodenhausen, G., Kogler, H., & Ernst, R. R. (1984) *J. Magn. Reson. 58*, 370−388.
Bradley, E. K., Thomason, J. F., Cohen, F. E., Kosen, P. A., & Kuntz, I. D. (1990) *J. Mol. Biol. 215*, 607−622.
Cavanagh, J., Fairbrother, W. J., Palmer, A. G., & Skelton, N. J. (1996) *Protein NMR Spectroscopy: Principles and Practice*, Academic Press, pp 1−587, San Diego.
Chen, W.-J., Goldstein, J. L., & Brown, M. S. (1990) *J. Biol. Chem. 265*, 3116−3123.
Chen, Y.-H., Yang, J. T., & Chau, D. H. (1974) *Biochemistry 13*, 3350−3359.
Chow, N., Korenberg, J. R., Chen, X.-N., & Neve, R. L. (1996) *J. Biol. Chem. 271*, 11339−11346.
Collawn, J. F., Stangel, M., Kuhn, L. A., Esekogwu, V., Jing, S., Trowbridge, I. S., & Tainer, J. A. (1990) *Cell 63*, 1061−1072.
Dyson, H. J., Rance, M., Houghten, R. A., Lerner, R. A., & Wright, P. E. (1988) *J. Mol. Biol. 201*, 161−200.
Fiore, F., Zambrano, N., Minopoli, G., Donini, V., Duilio, A., & Russo, T. (1995) *J. Biol. Chem. 270*, 30853−30856.
Frenkiel, T., Bauer, C., Carr, M. D., Birdsall, B., & Feeney, J. (1990) *J. Magn. Reson. 90*, 420−425.
Guenette, S. Y., Chen, J., Jondro, P. D., & Tanzi, R. E. (1996) *Proc. Natl. Acad. Sci. U.S.A. 93*, 10832−10837.
Halverson, K. J., Sucholeiki, I., Ashburn, T. T., & Lansbury, P. T. J. (1991) *J. Am. Chem. Soc. 113*, 6701−6703.
Harper, E. T., & Rose, G. D. (1993) *Biochemistry 32*, 7605−7609.
He, W., O'Neill, T. J., & Gustafson, T. A. (1995) *J. Biol. Chem. 270*, 23258−23262.
Ikura, M., Bax, A., Clore, G. M., & Gronenborn, A. M. (1990) *J. Am. Chem. Soc. 112*, 9020−9022.
Kang, J., Lemaire, H.-G., Unterbeck, A., Salbaum, J. M., Masters, C. L., Grzeschik, K.-H., Multhaup, G., Beyreuther, K., & Muller-Hill, B. (1987) *Nature 325*, 733−736.
Kirschner, D. A., Abraham, C., & Selkoe, D. J. (1986) *Proc. Natl. Acad. Sci. U.S.A. 83*, 503−507.
Kohno, T., Kobayashi, K., Tadakazu, M., Kazuki, S., & Takashima, A. (1996) *Biochemistry 35*, 16094−16104.
Koo, E. H., & Squazzo, S. L. (1994) *J. Biol. Chem. 269*, 17386−17389.
Kraulis, P. J. (1991) *J. Appl. Crystallogr. 24*, 946−950.
Lai, A., Sisodia, S. S., & Trowbridge, I. S. (1995) *J. Biol. Chem. 270*, 3565−3573.
Lansbury, P. T. J. (1996) *Acc. Chem. Res. 29*, 317−321.
Lansbury, P. T. J., Costa, P. R., Griffiths, J. M., Simon, E. J., Auger, M., Halverson, K. J., Kocisko, D. A., Hendsch, Z. S., Ashburn, T. T., Spencer, R. G. S., Tidor, B., & Griffin, R. G. (1995) *Nat. Struct. Biol. 2*, 990−998.
Lee, J. P., Stimson, E. R., Ghilardi, J. R., Mantyh, P. W., Lu, Y.-A., Felix, A. M., Llanos, W., Behbin, A., Cummings, M., Van

Criekinge, M., Timms, W., & Maggio, J. E. (1995) *Biochemistry 34*, 5191−5200.
Live, D. H., Davis, D. G., Agosta, W. C., & Cowburn, D. (1984) *J. Am. Chem. Soc. 106*, 1939−1941.
Marion, D., Ikura, M., & Bax, A. (1989a) *J. Magn. Reson. 84*, 425−430.
Marion, D., Ikura, M., Tschudin, R., & Bax, A. (1989b) *J. Magn. Reson. 85*, 393−399.
Merutka, G., Dyson, H. J., & Wright, P. E. (1995) *J. Biomol. NMR 5*, 14−24.
Messerle, B. A., Wider, G., Otting, G., Weber, C., & Wüthrich, K. (1989) *J. Magn. Reson. 85*, 608−613.
Nishimoto, I., Okamoto, T., Matsuura, Y., Takahashi, S., Okamoto, T., Murayama, Y., & Ogata, E. (1993) *Nature 362*, 75−79.
Palmer, A. G., Cavanagh, J., Byrd, R. A., & Rance, M. (1992) *J. Magn. Reson. 96*, 416−424.
Rance, M., Sørensen, O. W., Bodenhausen, G., Wagner, G., Ernst, R. R., & Wütrich, K. (1983) *Biochem. Biophys. Res. Com. 117*, 479−485.
Robakis, N. K., Ramakrishna, N., Wolfe, G., & Wisniewski, H. M. (1987) *Proc. Natl. Acad. Sci. U.S.A. 84*, 4190−4194.
Sambrook, J., Fritsch, E. F., & Maniatis, T. (1989) Molecular Cloning: a Laboratory Manual, Cold Spring Harbor Laboratory Press, Plainview, NY.
Selkoe, D. J. (1994) *Annu. Rev. Cell Biol. 10*, 373−403.
Selkoe, D. J. (1996) *J. Biol. Chem. 271*, 18295−18298.
Shaka, A. J., Lee, C. J., & Pines, A. (1988) *J. Magn. Reson. 77*, 274−293.
Songyang, Z., Margolis, B., Chaudhuri, M., Shoelson, S. E., & Cantley, L. C. (1995) *J. Biol. Chem. 270*, 14863−14866.
Talafous, J., Marcinowski, K. J., Klopman, G., & Zagorski, M. G. (1994) *Biochemistry 33*, 7788−7796.
Trowbridge, I. S., Collawn, J. F., & Hopkins, C. R. (1993) *Annu. Rev. Cell Biol. 9*, 129−161.
Wishart, D. S., Sykes, B. D., & Richards, F. M. (1991) *J. Mol. Biol. 222*, 311−333.
Wishart, D. S., Sykes, B. D., & Richards, F. M. (1992) *Biochemistry 31*, 1647−1651.
Wolf, G., Trub, T., Ottinger, E., Groninga, L., Lynch, A., White, M. F., Miyazaki, M., Lee, J., & Shoelson, S. E. (1995) *J. Biol. Chem. 270*, 27407−27410.
Wüthrich, K. (1986) *NMR of Proteins and Nucleic Acids*, pp 1−292, Wiley, New York.
Yamatsuji, T., Matsui, T., Okamoto, T., Komatsuzaki, K., Takeda, S., Fukmoto, H., Iwatsubo, T., Suzuki, N., Asami-Odaka, A., Ireland, S., Kinane, B., Giambarella, U., & Nishimoto, I. (1996) *Science 272*, 1349−1352.
Zambrano, N., Buxbaum, J. D., Minopoli, G., Fiore, F., De Candia, P., De Renzis, S., Faraonio, R., Sabo, S., Cheetham, J., Sudol, M., & Russo, T. (1997) *J. Biol. Chem. 272*, 6399−6405.
Zhou, M.-M., Ravichandran, K. S., Olejniczak, E. T., Petros, A. M., Meadows, R. P., Sattler, M., Harlan, J. E., Wade, W. S., Burakoff, S. J., & Fesik, S. W. (1995) *Nature 378*, 584−592.
Zhou, M.-M., Harlan, J. E., Wade, W. S., Crosby, S., Ravichandran, K. S., Burakoff, S. J., & Fesik, S. W. (1996) *J. Biol. Chem. 271*, 31119−31123.

BI9705669